Early lineage specification defines alveolar epithelial ontogeny in the murine lung

David B. Frank[a,b,c,1], Ian J. Penkala[d], Jarod A. Zepp[b,e], Aravind Sivakumar[a,b,c], Ricardo Linares-Saldana[c,d,e], William J. Zacharias[f], Katharine G. Stolz[a], Josh Pankin[a,b], MinQi Lu[a], Qiaohong Wang[c,d,e], Apoorva Babu[c,e], Li Li[c], Su Zhou[c], Michael P. Morley[b,c,e], Rajan Jain[c,d,e,1], and Edward E. Morrisey[b,c,d,e,1]

[a]Division of Pediatric Cardiology, Department of Pediatrics, Children's Hospital of Philadelphia, University of Pennsylvania, Philadelphia, PA 19104; [b]Penn Center for Pulmonary Biology, University of Pennsylvania, Philadelphia, PA 19104; [c]Penn Cardiovascular Institute, University of Pennsylvania, Philadelphia, PA 19104; [d]Department of Cell and Developmental Biology, Perelman School of Medicine, University of Pennsylvania, Philadelphia, PA 19104; [e]Department of Medicine, University of Pennsylvania, Philadelphia, PA 19104; and [f]Division of Pulmonary Biology, Department of Pediatrics, Cincinnati Children's Hospital, University of Cincinnati College of Medicine, Cincinnati, OH 45229

Edited by Brigid L. M. Hogan, Duke University Medical Center, Durham, NC, and approved January 23, 2019 (received for review August 13, 2018)

During the stepwise specification and differentiation of tissue-specific multipotent progenitors, lineage-specific transcriptional networks are activated or repressed to orchestrate cell specification. The gas-exchange niche in the lung contains two major epithelial cell types, alveolar type 1 (AT1) and AT2 cells, and the timing of lineage specification of these cells is critical for the correct formation of this niche and postnatal survival. Integrating cell-specific lineage tracing studies, spatially specific mRNA transcript and protein expression, and single-cell RNA-sequencing analysis, we demonstrate that specification of alveolar epithelial cell fate begins concomitantly with the proximal–distal specification of epithelial progenitors and branching morphogenesis earlier than previously appreciated. By using a newly developed dual-lineage tracing system, we show that bipotent alveolar cells that give rise to AT1 and AT2 cells are a minor contributor to the alveolar epithelial population. Furthermore, single-cell assessment of the transcriptome identifies specified AT1 and AT2 progenitors rather than bipotent cells during sacculation. These data reveal a paradigm of organ formation whereby lineage specification occurs during the nascent stages of development coincident with broad tissue-patterning processes, including axial patterning of the endoderm and branching morphogenesis.

lung development | alveolar epithelium | lineage fate | single-cell RNA sequencing

The precision of development depends on a stepwise lineage allocation of various cell lineages from multipotent progenitor cells. This progressive lineage restriction involves acquisition of cell fate-specific transcriptional programs and repression of alternative cell fate programs (1). Murine lung development follows similar paradigms and is initiated after specification of progenitor cells from the foregut endoderm at approximately embryonic day (E) 9.0 (2). Marked by expression of the transcription factor Nkx2.1, this multipotent endoderm progenitor undergoes lineage specification into $Sox2^+$ proximal and $Id2^+$/$Sox9^+$ distal endoderm progenitor cells before E13.5 (3–7). Following an axial patterning program of branching morphogenesis and growth, proximal and distal endoderm progenitor cells differentiate into the diverse lineages of the conducting airway and alveolar region, respectively.

Multilineage priming in progenitor cells is an emerging paradigm that is thought to exist in several organ systems and comprise a major mechanism for cell fate specification. As described in hematopoiesis, multilineage priming of hematopoietic stem cells (HSCs) provides plasticity for decision-making in commitment to several hematopoietic cell lineages (8–12). However, recent single-cell transcriptional profiling of HSCs suggests heterogeneity rather than synchronized specification and differentiation (13–16). Complementary studies using lineage tracing approaches, transplantation assays, and single-cell expression analyses have revealed that these populations exist as heterogeneous mixtures of unipotent, oligopotent, and transitioning progenitor cells that are lineage-restricted (15, 17–19).

A similar process of progressive lineage restriction has been proposed for lung alveolar epithelial cell lineage specification into alveolar type 1 (AT1) and AT2 cells from a $Sox9^+$/$Id2^+$ distal tip progenitor cell (6). An alternative model posits that alveolar epithelial cell specification occurs in a burst of activity during sacculation through a common bipotent alveolar epithelial progenitor cell (20, 21). However, there are few functional data available about a putative bipotent progenitor because of the lack of specific markers and appropriate tools to assess the fate of such a cell. In our previous study, we demonstrated that Wnt-responsive epithelial cells are found throughout the distal lung bud during branching morphogenesis and into sacculation, in which they were restricted to the AT2 fate (22). These data raised the possibility that alveolar epithelial cell fate is temporally restricted before the previously reported appearance of a bipotent progenitor cell (20, 21). In this report, we demonstrate that alveolar epithelial lineage specification begins earlier than previously appreciated, coincident with proximal–distal patterning and branching morphogenesis of the lung. These alveolar

Significance

Gas exchange requires the coordinated action of alveolar type 1 (AT1) and AT2 cells. AT1 cells promote gas exchange, and AT2 cells secrete surfactant proteins to reduce surface tension. However, the developmental ontology of these cells remains unclear. By using a combination of single-cell gene expression, single-cell RNA FISH, and combinatorial lineage-tracing methods, we show that the majority of AT1 and AT2 cells arise from progenitors expressing lineage-specific makers earlier than anticipated. We also identify cells expressing markers of both fates, and lineage tracing of these cells demonstrates a relatively small contribution to the mature alveolar epithelium.

Author contributions: D.B.F., A.S., R.L.-S., R.J., and E.E.M. designed research; D.B.F., I.J.P., J.A.Z., A.S., R.L.-S., W.J.Z., K.G.S., J.P., M.L., L.L., S.Z., R.J., and E.E.M. performed research; Q.W., R.J., and E.E.M. contributed new reagents/analytic tools; D.B.F., I.J.P., J.A.Z., A.S., W.J.Z., K.G.S., J.P., M.L., A.B., M.P.M., R.J., and E.E.M. analyzed data; and D.B.F., M.P.M., R.J., and E.E.M. wrote the paper.

The authors declare no conflict of interest.

This article is a PNAS Direct Submission.

Data deposition: The data reported in this paper have been deposited in the Gene Expression Omnibus (GEO) database, https://www.ncbi.nlm.nih.gov/geo (accession no. GSE113320).

[1]To whom correspondence may be addressed. Email: frankd@email.chop.edu, jainr@pennmedicine.upenn.edu, or emorrise@pennmedicine.upenn.edu.

This article contains supporting information online at www.pnas.org/lookup/suppl/doi:10.1073/pnas.1813952116/-/DCSupplemental.

Published online February 19, 2019.

progenitors restrict to AT1 or AT2 cell fates and arise from geographically distinct regions of the terminal branching airways, supporting their lineage separation in early lung development. Protein and gene-expression analyses combined with dual-recombinase lineage fate-mapping experiments reveal that cells expressing markers of AT1 and AT2 cells are rare, proliferate at a lower level than specified AT1 or AT2 precursors, and are akin to a developmental residual cell type that may lag in its differentiation state. Our data combining single-cell expression analyses, clonal lineage tracing, and a dual recombinase lineage-tracing allele reveal an alternative program of early lineage specification and differentiation in alveolar epithelial development coincident with the early major patterning events of lung development.

Results

Early SFTPC$^+$ and HOPX$^+$ Cells Are the Predominant Contributors to Alveolar Epithelial Development. Our previous data uncovered a sublineage of AT2s marked by active Wnt signaling (22). Surprisingly, cell fate mapping of this lineage indicated that this population gave rise to predominantly the AT2 lineage during sacculation, with only very rare AT1 progeny. Thus, we asked whether this was a characteristic specific to this lineage or if alveolar lineage specification programs are established much earlier in development. To assess this, we determined the relative contribution of AT1 and AT2 progenitor cells to the mature AT1 and AT2 lineages by using established AT1- and AT2-specific promoter-driven inducible Cre recombinases, *Hopx^{CreERT}* and *Sftpc^{CreERT2}* (23–27). We first assessed tamoxifen-independent recombination for each of the well established Cre recombinases and confirmed results previously reported in lung and other organs (23, 28, 29). Recombination was induced in *Hopx^{CreERT}:R26^{EYFP}* and *Sftpc^{CreERT2}:R26^{EYFP}* mice at E15.5 and E17.5, and animals were collected at the end of alveolarization at postnatal day (P) 30 and subsequently assessed with one of two AT1-specific markers (AQP5 and HOPX) and the canonical AT2 marker SFTPC. Quantification of more than 1,000 individual cells revealed that 84% of the HOPX$^+$ cells marked at E15.5 were specified to the AT1 cell lineage whereas 95% of the SFTPC$^+$ cells were specified to the AT2 lineage at this time (Fig. 1 *A–F* and *SI Appendix*, Fig. S1 *A–F*). By E17.5, 92% of HOPX$^+$ cells and more than 98% of SFTPC$^+$ cells were specified to the AT1 or AT2 lineages, respectively. We also performed short-term lineage tracing analysis; pregnant dams were induced with tamoxifen at E15.5, and embryos were analyzed at E17.5. In comparison with long-term labeling, we saw nearly equivalent results with the 48-h lineage tracing and confirming the fidelity of these alleles (*SI Appendix*, Fig. S1 *G–I*). Furthermore, we saw no specific pattern of specification in tiled images of whole lung lobes from these experiments (*SI Appendix*, Fig. S1 *J* and *K*). These data suggest that the vast majority of HOPX$^+$ and SFTPC$^+$ epithelial progenitor cells are specified to an AT1 or AT2 fate, respectively, before sacculation.

To define the clonal expansion of these specified AT1 and AT2 precursors, we performed lineage-tracing experiments by using low doses of tamoxifen and *R26$^{EYFP/+}$* or the multicolor genetic reporter *R26$^{Confetti/+}$* (23, 30). *Sftpc$^{CreERT2/+}$:R26$^{Confetti/+}$* pregnant dams were injected with a single dose of tamoxifen at E17.5, and animals were analyzed at P30. We scored the composition of clones by reconstructing stacks of confocal microscope images to ensure we scored clones fully extending into the *x–y–z* planes. Multicellular clones were almost completely composed of AT2, SFTPC$^+$ cells ($n = 42$ clones), with only a single AT1 clone observed (Fig. 1 *G–I*). In addition, the majority of clones were unicellular and AT2 ($n = 92$). We did not detect any clones that were a combination of AT1 and AT2 cells. On average, multicellular clones derived from the Sftpc$^+$ lineage were composed of 1.4 cells (*SI Appendix*, Fig. S1 *L* and *M*). As the *Hopx^{CreERT}* line inefficiently recombines the stop cassette in the *R26^{Confetti}* line, *Hopx^{CreERT}:R26^{EYFP}* pregnant dams were injected with a single limiting dose of tamoxifen at E17.5, and animals were also analyzed at P30. Of the 39 multicellular clones analyzed, 85% were composed entirely of AT1 cells and 5% were composed entirely of AT2 cells (Fig. 1 *J–L*). The remaining clones were composed of combinations of AT1 and AT2 cells. Multicellular clones arising from the Hopx$^+$ lineage were composed of an average of 1.4 cells (*SI Appendix*, Fig. S1 *L* and *M*). Together, these data suggest that the vast majority of specification to the AT1 and AT2 cell fate occurs pre-sacculation and is marked by early expression of Hopx and Sftpc, respectively.

Assessment of Alveolar Epithelial Cell Lineage Specification in Early Lung Development. During lung development, Id2 and Sox9 mark distal lung endoderm progenitor cells, and lineage tracing studies that used *Sox9^{CreERT2}* or *Id2^{CreERT2}* alleles suggest that distal lung tip progenitor cells give rise to AT1 and AT2 cells after E13.5 (6, 7, 27). To focus on the development of these distal alveolar endoderm progenitors, we employed a clonal cell fate-mapping strategy by using the *R26$^{Confetti/+}$* multicolor genetic reporter assay to assess when distal endodermal progenitor cells are specified to their respective fates. By using an inducible cre recombinase driven by the *Id2* gene (*Id2^{CreERT2}*) combined with *R26R^{Confetti}*, we labeled individual cells at various time points during early lung development with low doses of tamoxifen and analyzed multicellular clones at P0 (6, 31). Assessment of clones in cryosectioned optimal cutting temperature (OCT) compound-embedded tissue from *Id2^{CreERT2}:R26R^{Confetti}* embryos revealed that they were composed of AT1s, AT2s, or a mixture of AT1s and AT2s (*SI Appendix*, Fig. S2 *A–L*). More than 50% of the cells marked by *Id2^{CreERT2}* at E13.5 gave rise to clones composed of exclusively AT1 or AT2 cells (53% of 56 clones; *SI Appendix*, Fig. S2 *A–F* and *M*), and 75% of E15.5 Id2-labeled cells gave rise to AT1 or AT2 cells exclusively at P0 ($n = 48$ clones; *SI Appendix*, Fig. S2 *G–L* and *M*). *Id2^{CreERT2}*-labeled clone size resulted in slightly larger AT1/AT2 mixed clones at E13.5, but, by E15.5, single-lineage and multilineage clones were similar in size (*SI Appendix*, Fig. S2*N*).

To confirm these findings, we took an unbiased clonal cell fate-mapping strategy that labels all lung endodermal cells. Previous studies have demonstrated that Nkx2.1$^+$ cells give rise to the entirety of lung epithelium, including the alveolus, and that *Nkx2.1* is continuously expressed throughout the lung epithelium during development (32). These studies have been interpreted to mean that a multipotent Nkx2.1$^+$ cell gives rise to the multiple cell types of the lung, but, to the best of our knowledge, a detailed clonal analysis has not yet been reported. By using an inducible Cre recombinase driven by the *Nkx2.1* gene (*Nkx2.1^{CreERT2}*) combined with the Rosa26 Confetti reporter (*R26R^{Confetti}*), we labeled individual cells at E13.5 and E15.5 with low doses of tamoxifen and again analyzed multicellular clones at P0 (Fig. 2 and *SI Appendix*, Fig. S3 *A–I*) (31, 33). In this set of experiments, we used thicker sections than for the *Id2^{CreERT2}* experiments to capture the entire clone size where possible (Fig. 2 *A–F* and *SI Appendix*, Fig. S3*G*). As expected with the use of this technique, *Nkx2.1^{CreERT2}:R26R^{Confetti}* clones were larger than observed in the *Id2^{CreERT2}:R26R^{Confetti}* embryos. Despite these size differences, we still observed clones comprised of a single alveolar epithelial lineage (AT1 or AT2) at E13.5 ($n = 44$ clones; Fig. 2 *A–C* and *G*). By E15.5, 70% of the *Nkx2.1^{CreERT2}:R26R^{Confetti}*-derived clones in the lung alveolus were composed exclusively of AT1 or AT2 cells ($n = 46$ clones; Fig. 2 *D–G*). In addition, confirmation of alveolar cellular identity depicted via positive or negative SFTPC expression was performed on 16-μm paraffin-embedded sections with antibodies specific for fluorescent proteins, SFTPC, and AQP5 (*SI Appendix*, Fig. S3 *A–F*). We also assessed absolute cell numbers in clones. At E13.5, mixed

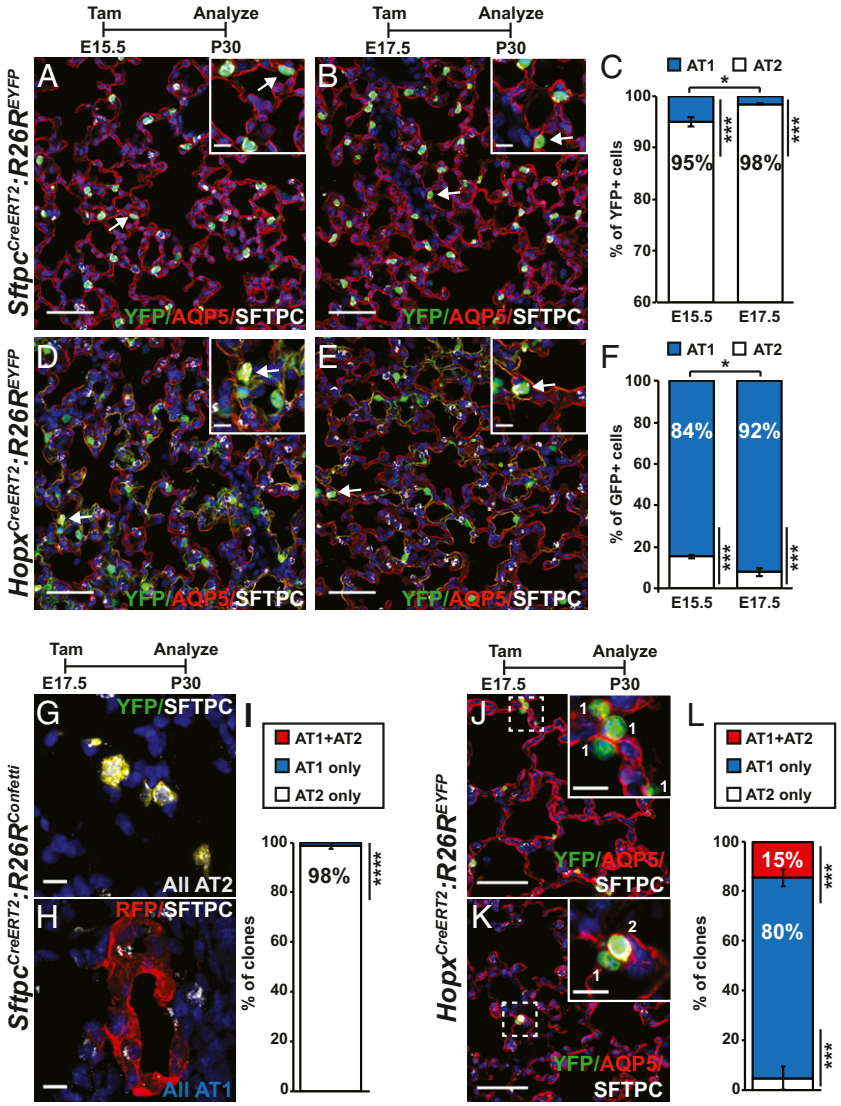

Fig. 1. Lineage tracing of alveolar progenitors reveals early lineage commitment. (*A* and *B*) *Sftpc*^{CreERT2}:*R26R*^{EYFP} pregnant dams were injected with tamoxifen at E15.5 (*A*) or E17.5 (*B*), and animals were analyzed at P30. Tissue was stained for YFP, AQP5, and SFTPC. Cells highlighted by arrows are magnified in the *Insets*, and are examples of rare lineage-traced cells expressing AQP5. (*C*) Quantification of lineage tracing displaying percentage of lineage-traced cells that were AT1 (HOPX$^+$) or AT2 (SFTPC$^+$) cells ($n \geq 1{,}300$ cells quantified at each time point). (*D* and *E*) *Hopx*^{CreERT}:*R26R*^{EYFP} pregnant dams were injected with tamoxifen at E15.5 (*D*) or E17.5 (*E*), and animals were analyzed at P30. Tissue was stained for YFP, AQP5, and SFTPC. Cells highlighted by arrows are magnified in the *Insets*, and are examples of rare lineage-traced cells expressing SFTPC. (*F*) Quantification of lineage tracing displaying percentage of lineage-traced cells that were AT1 (HOPX$^+$) or AT2 (SFTPC$^+$) cells ($n \geq 460$ cells quantified at each time point). (*G* and *H*) *Sftpc*^{CreERT2}:*R26R*^{Confetti} pregnant dams were injected with tamoxifen at E17.5, and embryos were analyzed at P0. (*G*) YFP$^+$ clone of AT2 cells (marked by Sftpc) and (*H*) RFP$^+$ clone of AT1 cells. (*I*) Quantification of clonal analysis ($n = 43$ clones). (*J*–*K*) *Hopx*^{CreERT}:*R26R*^{EYFP} pregnant dams were injected with tamoxifen at E17.5, and animals were analyzed at P0. Tissue was stained with SFTPC and AQP5. Clones marked by YFP composed of AT2 SFTPC$^+$ cells are shown (highlighted in box and magnified in *Insets*). (*L*) Quantification of clonal analysis [$n = 41$ multicellular clones; *$P < 0.05$, **$P < 0.01$, and ****$P < 0.0001$ by two-tailed *t* test (*C*, *F*, horizontal and vertical bars) or ANOVA (*I* and *L*)]. [Scale bars: *A*, *B*, *D*, and *E*, 50 μm; *J* and *K*, 25 μm; and *G*, *H*, *A* (*Inset*), *B* (*Inset*), *D* (*Inset*), *E* (*Inset*), *J* (*Inset*), and *K* (*Inset*), 10 μm.]

AT1/AT2 clones contained a higher number of cells than AT2- or AT1-only clones, and this difference was significantly reduced by E15.5, possibly reflecting a significant reduction in proliferation of multilineage clones between these two time points (Fig. 2*H*). As immunostaining of thick sections is less efficient, which could lead to a loss of staining for some cells, we used a slightly less stringent clonal composition of greater than or equal to 90% AT1-only or AT2-only cells to quantify clonal composition. This analysis reveals that 46% of Nkx2-1$^+$ cells give rise to a single lineage (>90%) by E13.5 (*SI Appendix*, Fig. S3*H*). This analysis also shows that clone sizes were similar between mixed AT1/AT2 and AT2-only clones, but both of these were larger than the AT1-only clones (*SI Appendix*, Fig. S3*I*). Taken together, these clonal fate-mapping studies indicate that many Nkx2-1 and Id2 cells undergo lineage specification into AT1 or AT2 cells by E13.5, earlier than previously appreciated (20, 21).

These data raised the possibility that a surprising number of Nkx2-1$^+$ lung endodermal progenitors are committed to a fate by E13.5. Given this finding, we assessed fate at an earlier time point in lung development to examine temporal acquisition of cell-specific alveolar fate. Similar to previous studies on early lung endoderm, cells labeled at E11.5 gave rise to clones of diverse composition, including proximal and distal cell fates (*SI Appendix*, Fig. S3 *J* and *K*) (6). Although we did identify alveolar-only

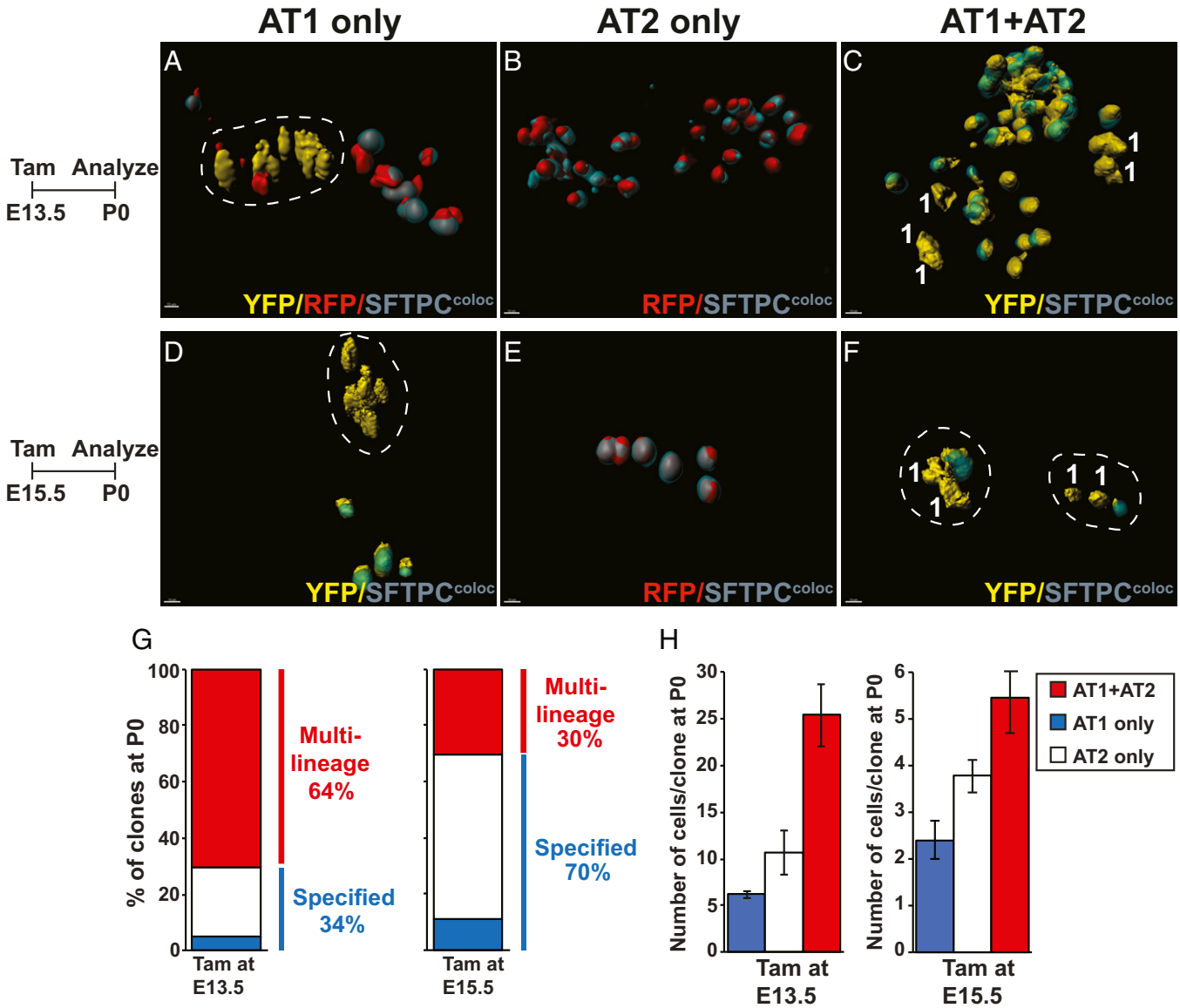

Fig. 2. Clonal lineage tracing of Nkx2-1$^+$ lung embryonic alveolar progenitors in thick sections. (*A–C*) *Nkx2.1*^{CreERT2}:*R26R*^{Confetti} pregnant dams were injected with tamoxifen at E13.5, and embryos were analyzed at P0. Analysis revealed single color clones of cells composed of AT1 cells (*A*), AT2 cells (*B*), or both cell types (*C*). (*D–F*) *Nkx2.1*^{CreERT2}:*R26R*^{Confetti} pregnant dams were injected with tamoxifen at E15.5, and embryos were analyzed at P0 (*E*). Alveolar epithelial clones comprising AT1 cells (*D*), AT2 cells (*E*), and both cell types were identified (*F*). Histology on 150-μm tissue sections counterstained with SFTPC, processed for colocalization with fluorescent proteins, 3D surface-rendering using Imaris, and represented in images as SFTPC colocalization in teal/gray color. Cells were manually highlighted and marked as AT2 cells if they expressed SFTPC and AT1 cells if they did not. (*G* and *H*) Quantification of clonal analysis including clone composition and clone size of Nkx2.1$^+$ cells at E13.5 and E15.5 (n = 46 and n = 44 clones, respectively). Mixed AT1/AT2 clones include any combination less than 100% pure AT1- or AT2-only clones. (Scale bars, *A–F*, 10 μm.)

lineage-containing clones, these clones were generally a mixed population of AT1 and AT2, and these experiments suggest that the lung endoderm is comprised of oligopotent progenitors at this early stage (*SI Appendix*, Fig. S3 *L* and *M*). Together, these data suggest that alveolar epithelial lineage specification occurs as early as E13.5.

Alveolar Epithelial Lineage Specification Coincides with Axial Patterning of the Lung Endoderm. To better define the relationship of alveolar lineage specification to axial or proximal-distal patterning, we compared HOPX and SFTPC expression vs. the early proximal and distal progenitor cell markers SOX2 and SOX9, respectively. HOPX expression delineates two domains within the lung bud at E15.5, a proximal HOPX$^+$/SOX2$^+$ population and a region of HOPX$^+$/SOX9$^-$/SOX2$^-$ expression in the stalk of the lung bud adjacent and just proximal to the SFTPC-expressing domain (Fig. 3 *A–C*). In contrast, SFTPC expression is generally confined to the SOX9$^+$ progenitor compartments with little overlap between SFTPC and HOPX in the SOX9$^+$ distal tip at E15.5 (Fig. 3 *B* and *C* and *SI Appendix*, Fig. S4*A*). A similar but more restricted pattern occurs at E17.5. HOPX expression is confined to the area of the stalk with very little overlap with SOX2 and SFTPC (Fig. 3 *D* and *E*). Quantification of single- and mixed-cell lineage numbers expressing HOPX or SFTPC was also performed. At E15.5, only 7% of cells express HOPX and SFTPC, with equal numbers of SFTPC$^+$-only and HOPX$^+$-only cells (Fig. 3*F*). Although there are rare HOPX$^+$/SFTPC$^+$ cells in the distal region of the airways at

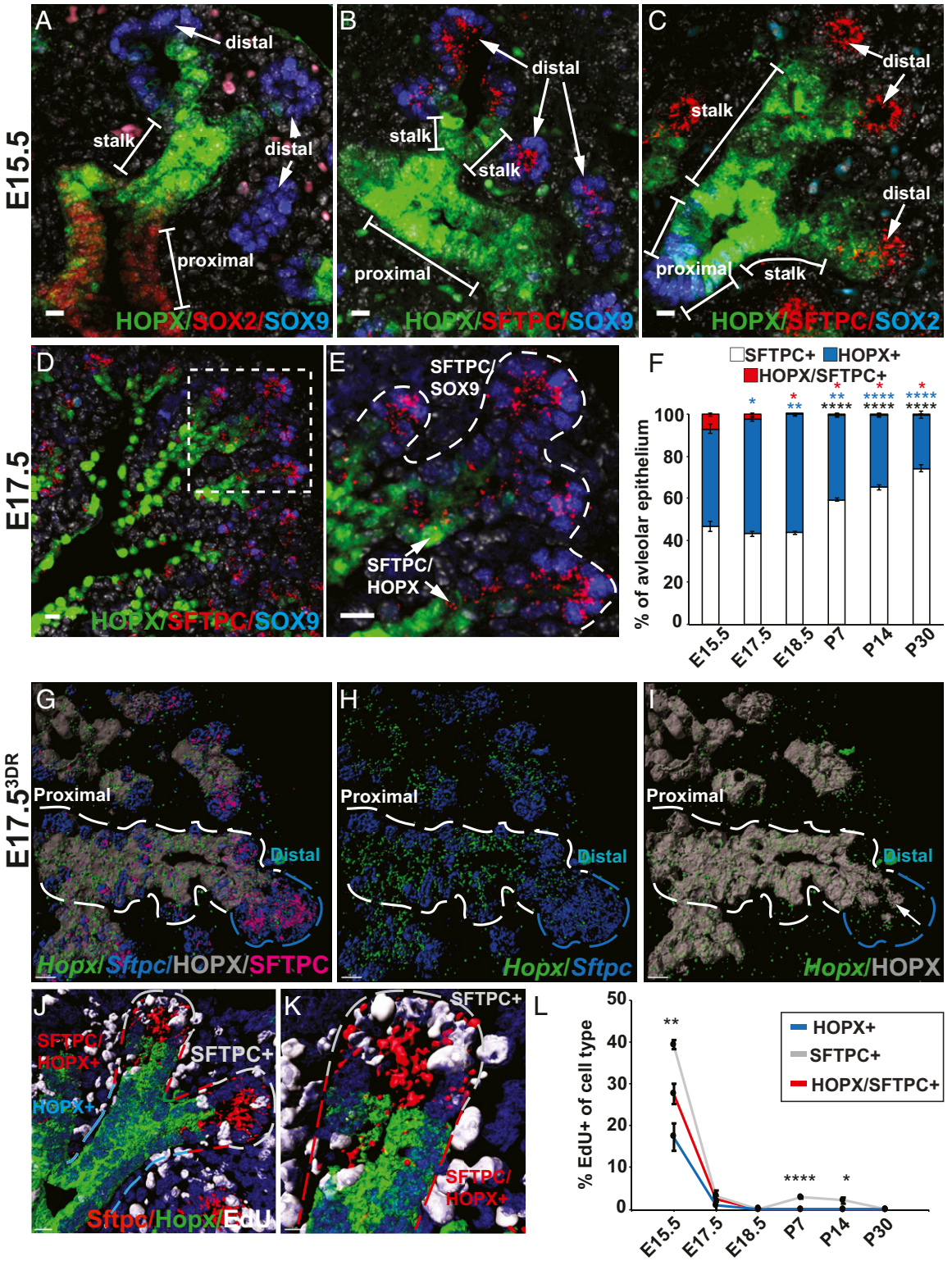

Fig. 3. Spatial restriction of distal lung embryonic progenitors. (*A*) HOPX, SOX2, and SOX9 staining in E15.5 lung tissue. Distal tip, stalk, and proximal portion of lung bud are denoted. (*B*) HOPX, SFTPC, and SOX9 staining in E15.5 lung tissue. (*C*) HOPX, SFTPC, and SOX2 staining in E15.5 lung tissue. (*D*) HOPX, SFTPC, and SOX9 staining in E17.5 lung tissue. (*E*) Higher magnification of boxed area in *D*. HOPX, SOX2, and SOX9 staining in E17.5 lung tissue. Distal tip cells indicated with white dotted line and arrows indicate cells expressing HOPX and SFTPC. (*F*) Quantification of cells expressing indicated proteins at indicated time points. Red asterisk indicates the difference in bilineage population compared with E15.5. Blue asterisk indicates the difference in AT1 population. Black asterisk indicates the difference in AT2 population. (*G–I*) Localization of *Hopx* and *Sftpc* transcript levels relative to HOPX and SFTPC protein expression in E17.5 lung tissue. Distal and proximal domains are marked by blue and white dashed lines, respectively. White arrow indicates rare cell expressing Hopx and Sftpc protein and mRNA. (*J* and *K*) E15.5 lung tissue stained with SFTPC, HOPX, and Edu. Animals were injected with Edu (50 mg/kg) 4 h before euthanasia (3D resconstruction images). The developing alveoli are outlined with the dotted line. Blue represents cells expressing HOPX, gray represents cells expressing Sftpc, and red indicates cells marked by SFTPC and HOPX. (*L*) Quantification of percentage of indicated cells that were Edu$^+$ at indicated time points ($n \geq 1{,}800$ cells quantified at each time point; $^*P < 0.05$, $^{**}P < 0.01$, and $^{****}P < 0.0001$ by ANOVA). (Scale bars, 10 μm.)

E17.5 (less than 2%), the vast majority of the distal tip cells are exclusively SFTPC$^+$.

A previous study identified a prevalent population of bipotent alveolar cells based on single-cell RNA sequencing (scRNA-seq) (21). However, recent studies indicate that the abundance of mRNA transcripts and protein expression do not always correlate, especially at the single-cell level (34, 35). Therefore, we characterized the simultaneous expression of protein and mRNA of Hopx and Sftpc during alveolar epithelial cell specification. We performed RNA FISH combined with protein immunohistochemistry on tissue sections to colocalize *Hopx* and *Sftpc* mRNA and HOPX and SFTPC protein. We first confirmed specificity of RNA FISH probes in WT and KO tissue (*SI Appendix*, Fig. S4 *B–E*). At E15.5, *Hopx* is expressed primarily in the stalk region, with reduced expression in the distal tip, where *Sftpc* is most abundant (*SI Appendix*, Fig. S4 *F–H*). However, HOPX protein is almost completely restricted to the stalks of the lung bud at this time. By E17.5, *Sftpc* transcript and SFTPC protein are confined to the distal tip cells, with only a few rare SFTPC/HOPX-coexpressing cells confined to the more proximal stalk region (Fig. 3 *G–I*). *Hopx* transcript and protein are highly correlated and expressed in the stalk region at this stage, with rare *Hopx*/HOPX expression noted in a few Sftpc$^+$ cells in the very distal bud of the stalk.

To determine whether there is preferential cell proliferation in such rare SFTPC$^+$/HOPX$^+$ cells compared with SFTPC$^+$- or HOPX$^+$ only cells, we also performed EdU incorporation assays to quantify the number of cells undergoing DNA synthesis and thus cell proliferation. We compared the total number of HOPX$^+$, SFTPC$^+$, and SFTPC$^+$/HOPX$^+$ cells within the distal airways at multiple time points across development and compared this vs. the EdU-defined proliferation rate of these cell types (Fig. 3 *J–L* and *SI Appendix*, Fig. S4 *I–R*). We detected rare SFTPC$^+$ HOPX$^+$ cells, which were labeled by Edu at E15.5, whereas labeled SFTPC$^+$ or HOPX$^+$ cells were readily observed. SFTPC$^+$/HOPX$^+$ cells diminish rapidly, such that by E18.5 they represent less than 1% of the total developing alveolar epithelium. As expected, proliferation rates in all three cell types were highest at E15.5, with the SFTPC$^+$ cells exhibiting a slight increase during postnatal alveolarization as previously reported (22). However, at all time points examined, the proliferation rate for SFTPC$^+$/HOPX$^+$ cells was lower than that for SFTPC$^+$ cells. These data indicate that SFTPC$^+$/HOPX$^+$ putative bilineage cells exist but likely represent a very small minority population compared with specified AT1 (HOPX$^+$) or AT2 (SFTPC$^+$) lineages, and they do not preferentially proliferate compared with these specified lineages.

Single-Cell Transcriptome Reveals Decreasing Heterogeneity and Increasing Lineage Specification During Alveolar Epithelial Development. Our clonal analysis suggests a heterogeneous pool of NKX2-1$^+$/ID2$^+$ endoderm progenitor cells in early lung development that are progressively specified to specific alveolar epithelial lineages between E11.5 and E13.5, a process that is mostly complete by E17.5. To further delineate this heterogeneity and characterize endoderm heterogeneity at the time the bipotent cell population is reported to exist, we examined the totality of lung endoderm by using scRNA-seq transcriptome analysis of *Nkx2-1*$^{GFP/+}$ cells at E17.5. scRNA-seq analysis has been used to assess heterogeneity and assign subpopulation relationships in multipotent progenitor and differentiated cell populations (14, 15, 17–19, 21, 36, 37). A total of 7,106 isolated NKX2.1$^+$ cells were subjected to scRNA-seq analysis by using the in-drop/10× Genomics method (38). By using graph-based clustering, we identified 11 distinct clusters at E17.5 and visualized the results using t-distributed stochastic neighbor embedding (tSNE; Fig. 4*A*). Most of these clusters could be readily assigned to known epithelial cell lineages, including AT1, AT2, multiciliated epithelial cells, secretory epithelial cells, and neuroendocrine cells. Also included in this clustering algorithm were a cluster of presumably contaminating endothelial cells, a cluster representing proliferating cells across different cell types, and a cluster exhibiting a stress response that was also represented across different cell types (Fig. 4*A* and *SI Appendix*, Fig. S5). The stress-induced and proliferation clusters express slightly higher levels of AT1 but not AT2 markers. The proliferation and stress-induced clusters were not used in further analysis because of their specialized gene-expression program. Hierarchical clustering of the differentially expressed genes revealed clear differences between different clusters, representing the different epithelial cell lineages in the lung at E17.5 (Fig. 4*B*). Classifying clusters based on statistically significant enrichment for known marker genes of AT1 and AT2 cells, we identified four clusters likely representing AT1 or AT2 cells at differing levels of differentiation (Fig. 4 *A*, *C*, and *D* and *SI Appendix*, Fig. S5). Based on differential gene expression and levels of expression of genes in differentiated alveolar cell types, we further classified these as likely representing AT1 precursor cells (cluster 1), AT1 cells (cluster 2), AT2 precursor cells (cluster 3), and AT2 cells (cluster 4). If our cluster assignment was correct, cells should order themselves in a pseudotime analysis reflecting precursor cell specification into differentiated cell types. Therefore, we analyzed our single-cell transcriptome data by using Monocle2 (39), and indeed cells ordered themselves as predicted by our clusters. These analyses also suggested that the AT1 and AT1-precursor cluster and the AT2 and AT2-precursor clusters exhibited distinct and unique states (Fig. 4 *E* and *F*). This was supported by enhanced expression of genes known to be highly expressed in more mature or differentiated AT2 cells, such as *Sftpa1*, *Sftpb*, and *Lamp3* for AT2 cells and *Aqp5* for more mature AT1 cells (Fig. 4 *C* and *D*). Although there is some gene expression overlap of AT1 and AT2 markers across the various cell clusters, these data are consistent with our lineage-tracing studies and demonstrate that the cells exhibiting an AT1 or AT2 gene-expression program are specified to their respective fates by E17.5 based on scRNA-seq analysis.

A Dual-Lineage Tracing System Reveals That HOPX/SFTPC$^+$ Cells Do Not Significantly Contribute to Formation of the Lung Alveolus. Our data suggest that cells expressing SFTPC and HOPX are rare, have limited proliferation potential, and do not significantly contribute toward alveolar epithelial cell differentiation. To further validate this concept, we developed and employed a dual-lineage tracing approach to define the fate of cells expressing markers of the AT1 (HOPX) and AT2 (SFTPC) cell lineages. We combined an allele expressing a tamoxifen-inducible Cre recombinase under control of the *Sftpc* promoter (*Sftpc*^{CreERT2}) and a new allele expressing a tamoxifen-inducible codon-optimized version of Flp recombinase under the control of the *Hopx* promoter (*Hopx*$^{FlpoERT/+}$; Fig. 5*A*). We confirmed activity of both of these alleles by using traditional Cre and Flp-dependent TdTomato lineage reporters (Fig. 5 *B* and *C*). Both of these mouse lines were then crossed into a reporter line harboring a Cre and Flp dual-dependent TdTomato cassette (*R26*$^{RCFL\text{-}TdTom}$), whereby TdTomato expression occurs only in the presence of two simultaneously active promoters driving both Cre and Flp recombinase (40). Mice injected with corn oil did not exhibit any lineage tracing. We induced pregnant dams at E15.5 with tamoxifen and analyzed lungs at P0 (Fig. 5*D*). We found scattered clones largely composed of one to three cells, in accord with the aforementioned proliferation data (Fig. 5 *E–G*). Consistent with the relative small contribution of double-labeled cells, we isolated *Nkx2-1*$^{GFP/+}$ cells at E15.5 and observed that 21.1% were *Sftpc*$^+$, 14.2% were *Hopx*$^+$, and 4.6% were *Sftpc*$^+$ *Hopx*$^+$ (*SI Appendix*, Fig. S6). Approximately 63% of these multicellular clones in our dual-lineage tracing experiments were composed of only AT1 or AT2 cells, with 37% of clones composed of both AT1 and AT2 cells (n = 32; Fig. 5*H*). Although

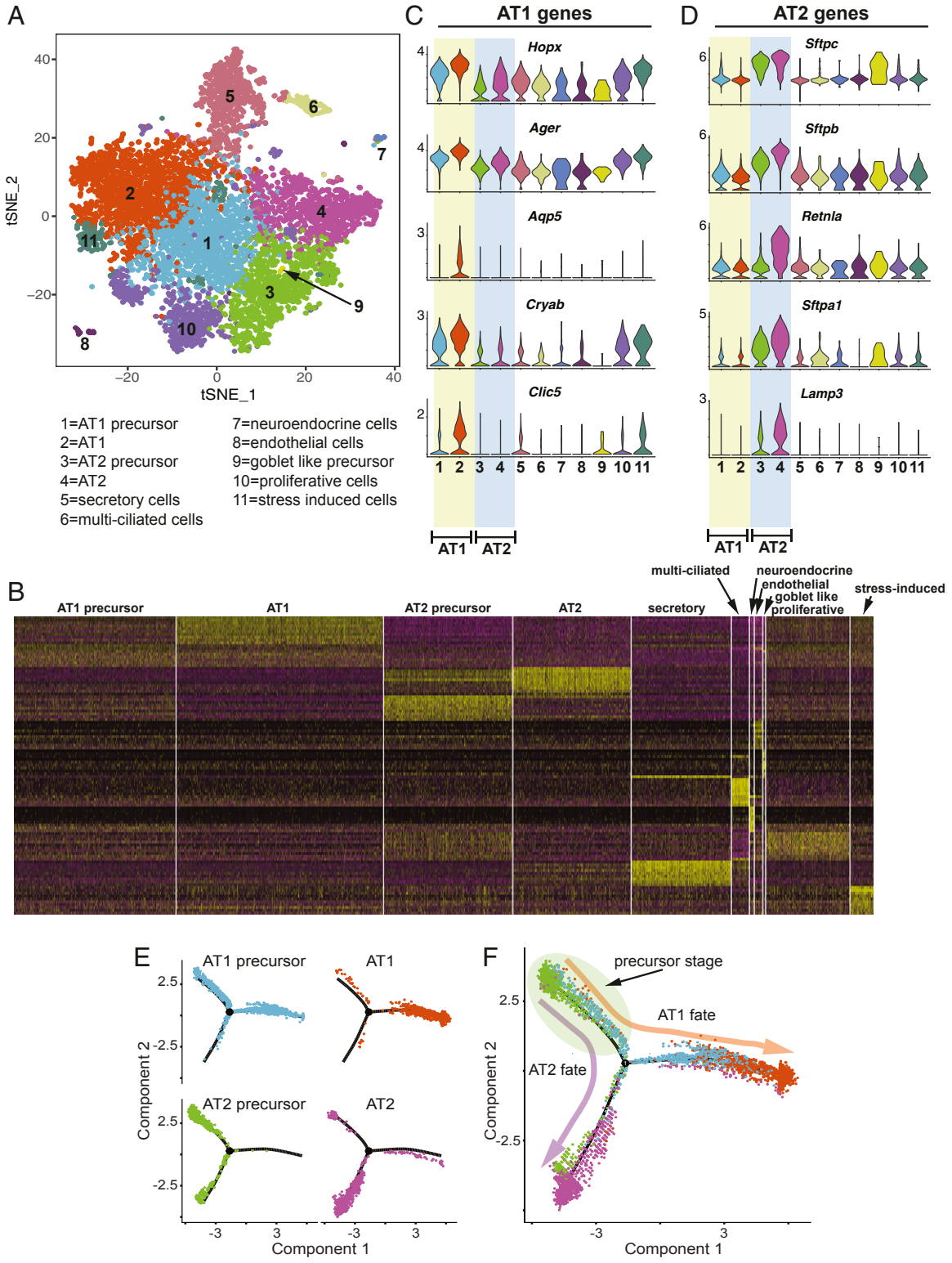

Fig. 4. Single-cell transcriptome data demonstrate that the AT1 and AT2 cell fates are specified by E17.5. (*A*) tSNE plot of 7,106 Nkx2.1^{+} cells from E17.5 lungs revealing 11 distinct clusters. Each cluster marks a distinct cell type as shown. (*B*) Heat map of the top differentially expressed genes showing distinct gene expression signatures in each of the 11 clusters. (*C*) Violin gene-expression plots for five of the AT1 differentially expressed genes across all of the 11 clusters as defined under tSNE plot. (*D*) Violin gene-expression plots for five of the AT2 differentially expressed genes across all of the 11 clusters as defined under tSNE plot. (*E*) Pseudotime analysis of the AT1, AT1 precursor, AT2, and AT2 precursor clusters showing distinct cell trajectories and connection between the precursor and more mature state of each cell lineage. (*F*) Overlay of the pseudotime analysis indicating the AT1 and AT2 cell fate trajectories and the precursor stage in the upper left branch.

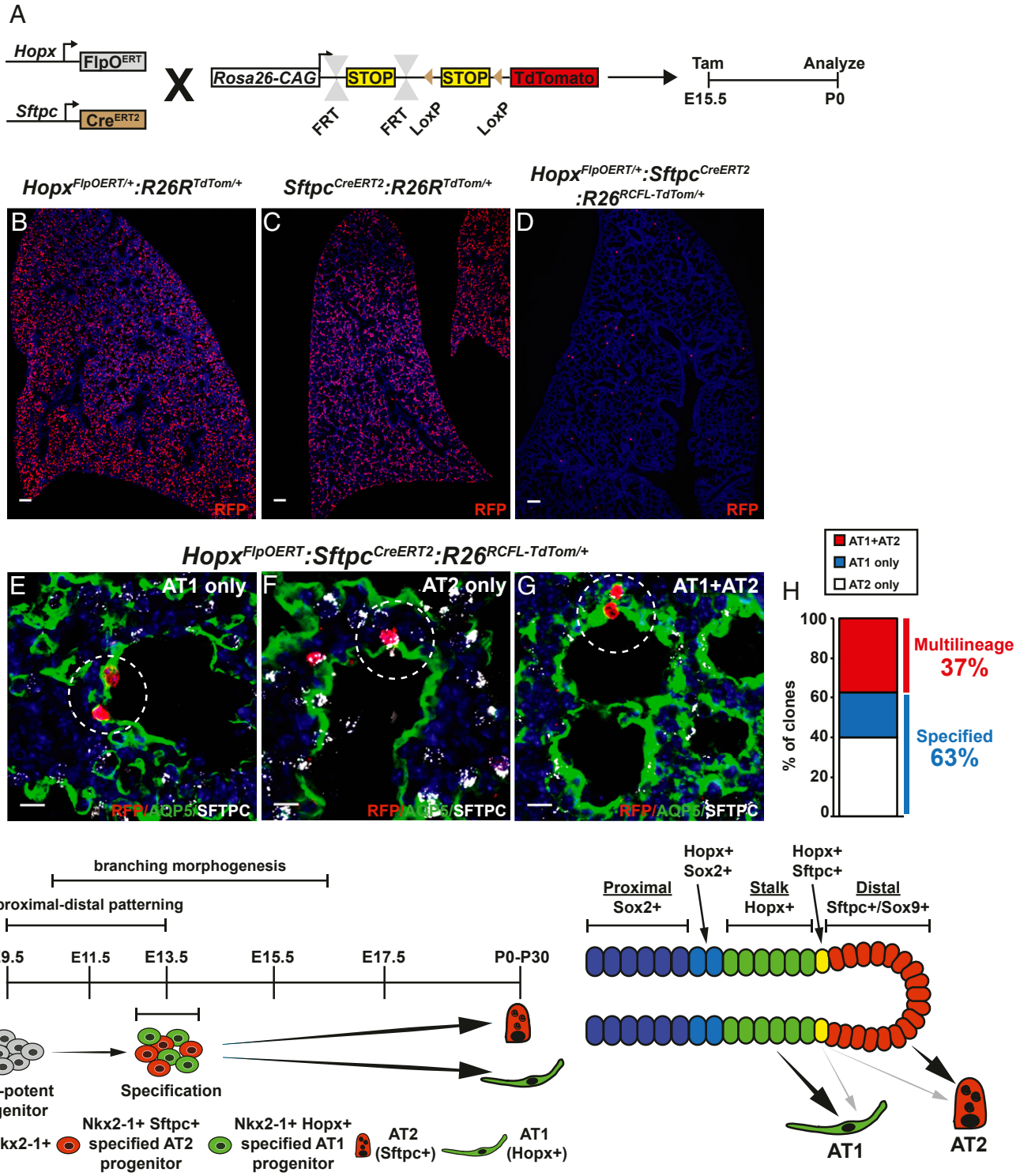

Fig. 5. Dual-lineage tracing demonstrates minimal contribution of Hopx$^+$/Sftpc$^+$ bilineage cells. (*A*) Schema of dual-lineage tracing using the *R26*$^{RCFL\text{-}TdTom}$ allele. (*B*) *Hopx*$^{FlpoERT/+}$:*R26R*$^{TdTom/+}$ pregnant dams were injected with tamoxifen at E15.5, and animals were analyzed at P0; lineage-traced RFP$^+$ cells are shown. Of note, the *R26R*$^{RCFL\text{-}TdTom/+}$ lineage reporter used in this experiment had previously been bred to a CMV-Cre mouse to excise the floxed cassette to generate an flp-only RFP reporter. (*C*) *Sftpc*^{CreERT2}:*R26R*^{TdTom} pregnant dams were injected with tamoxifen at E15.5, and animals were analyzed at P0; lineage-traced RFP$^+$ cells are shown. (*D*) *Hopx*$^{FlpoERT/+}$:*Sftpc*^{CreERT2}:*R26R*$^{RCFL\text{-}TdTom}$ pregnant dams were injected with tamoxifen at E15.5, and animals were analyzed at P0. (*E* and *G*) Clones of AT1 cells (*E*), AT2 cells (*F*), and both AT1 and AT2 cells (*G*) were identified when sections from *Hopx*$^{FlpoERT/+}$:*Sftpc*^{CreERT2}:*R26R*$^{RCFL\text{-}TdTom}$ were stained with RFP, AQP5, and SFTPC. (*H*) Quantification of clone identity ($n = 45$ clones). (*I*) Model illustrating early specification of alveolar epithelial progenitors (*$P < 0.05$ by two-tailed t test). (Scale bars: *B–D*, 50 μm; *E–G*, 10 μm.)

this dual-recombinase system cannot be directly compared with single cre recombinase lineage tracing systems as described here earlier, the finding that 37% of this rare population can generate both AT1 and AT2 cells is consistent with the data shown in Fig. 1. These data indicate that the vast majority of AT1 and AT2 cells are specified by E15.5 and that cells expressing both HOPX and SFTPC contribute to only a small minority of cells within the mature alveolus (Fig. 5*I*).

Discussion

The timing and extent of lineage specification can affect multiple aspects of tissue development and regeneration. Our data reveal that lung alveolar epithelial cell specification occurs remarkably early in development, coincident with major organ patterning processes such as proximal–distal axial patterning and branching morphogenesis of the airways. By using clonal and dual-recombinase reporter systems combined with cell-specific RNA and protein expression and scRNA-seq analysis, we reveal that this early specification occurs within a heterogeneous population of NKX2-1$^+$ alveolar epithelial progenitors. Our studies demonstrate a remarkable level of endodermal heterogeneity during critical times of alveolar development, with a mixture of multipotent progenitor cells, specified progenitor cells, and differentiated cells. Although there are limits to our dual-recombinase strategy, the relative minimal contribution of SFTPC$^+$/HOPX$^+$ cells at multiple time points suggest that alveolar epithelial lineages arise largely from a unilineage-primed progenitor cell rather than multi-, oligo-, or bilineage progenitor cells.

Recent single-cell analyses in the hematopoietic system and cardiac development have demonstrated extensive heterogeneity of progenitor pools and the existence of lineage-restricted progenitors (13–16, 41), revising our understanding of progressive lineage restriction in tissue development. For instance, pioneering studies using embryonic stem cell (ESC) differentiation strategies identified multipotent progenitors during cardiac development (42–45). However, more recent studies using inducible lineage-tracing approaches in vivo have found that the heart arises largely from unipotent and oligopotent progenitors (46, 47). Likewise, sophisticated lineage-tracing studies employed during hematopoietic development and maintenance point to a similar paradigm (15).

The differences observed between the in vitro systems and in vivo studies may be rooted in cellular competence, including the ability of a cell to specifically and dynamically respond to an inductive cue (48, 49). As described here earlier, even though ESC differentiation studies suggest that progenitor cells, outside of their native context, are competent to differentiate into multiple cardiac cell types, this lineage plasticity is far more constrained in vivo. A similar paradigm has been observed in skin and hair follicle differentiation. Lrig$^+$ cells give rise to interfollicular epidermis and sebaceous glands in vivo, but, upon transplantation, are competent to give rise to all of the epidermal lineages (50). Context-dependent regulation of cellular plasticity and fate has also been observed in previous studies of lung epithelial differentiation. In the setting of severe injury in in vivo models and ESC differentiation studies in 2D models, alveolar cells gain plasticity and the ability to differentiate into AT1 and AT2 lineages (24, 30, 51–54). However, in more native niches of in vivo lung development and in vitro human ESC differentiation into 3D lung alveolar epithelial cell organoids, alveolar epithelial cells are largely lineage-restricted (22, 53). Importantly, SFTPC$^+$/HOPX$^+$ cells do not exhibit a higher level of proliferation after E15.5 compared with cells expressing only a single lineage marker. This indicates that such bipotent cells are unlikely to populate the developing alveolus over the more unipotent cells.

Recognizing the limitations of any recombinase-based lineage tracing system, including potential unforeseen bias in cells which are labeled, our data support a similar program in which a significant number of NKX2-1$^+$ multipotent endodermal progenitor cells are primed toward a particular alveolar cell fate early in development. It will be interesting to apply emerging unbiased barcoding strategies to lineage trace all cells in vivo, circumventing bias in existing lineage tracing approaches (55). Sequential barcoding strategies, building on a recently published CellTag strategy, could provide an understanding of whether waves of specification and differentiation occur (56). However, it will be important to pair these approaches with assays that do not lose spatial-resolution information of derived cells. Regardless, these results reinforce the importance of defining the molecular determinants of lineage specification. A particularly exciting area of research is how mechanical forces influence cell differentiation. Recently, it has been shown that mechanical forces promote the AT1 differentiation, whereas AT2 progenitors are shielded from these forces by a niche cell (57). It will be important to determine if and how mechanical forces induce specification of cell type as opposed to reinforcing cell fate, again highlighting the importance of understanding the mechanisms underlying cellular competence. Such mechanical forces may also help explain how AT1 and AT2 cells migrate into and intermix within the mature alveolus even though they are initially specified in different zones of the distal branching airways.

We propose a paradigm for alveolar cell commitment in which specific cell fates are initiated early in NKX2-1$^+$/ID2$^+$ endodermal progenitors coincident with proximal–distal patterning and branching morphogenesis of the endoderm. Spatial segregation of AT1 and AT2 precursors exists throughout early lung development, with most AT2 cells arising from the highly proliferative SOX9$^+$ most distal tip endodermal population and AT1 cells from a region just proximal to this in the stalk of the lung bud. The small number of bilineage AT1/AT2 cells that exist between these two regions may represent residual undifferentiated progenitor cells, which progressively differentiate during development and do not contribute in a significant manner to mature alveolar epithelial lineages.

Materials and Methods

Animals. *Nkx2.1*^{CreERT2} (33), *Id2*^{CreERT2} (6), *Nkx2.1*^{GFP} (38), *Hopx*^{CreERT} (24), *Sftpc*^{CreERT2} (23), *Sox2*^{CreERT2} (58), *R26R*^{EYFP} (59), *R26R*^{Confetti} (31), and *R26*$^{RCFL\text{-}TdTom}$ (40) mice have been previously described. All animal studies were completed under the guidance of the University of Pennsylvania Institutional Animal Care and Use Committee.

Lineage Tracing. To induce recombination, a solution consisting of tamoxifen (Sigma) dissolved in 100% ethanol and diluted with corn oil (Sigma) for a 10% ethanol:corn oil:tamoxifen mixture at 20 mg/mL was used. Pregnant dams were injected i.p. with limiting doses of the tamoxifen mixture dependent on the efficiency of each inducible Cre and reporter mouse line. The *R26R*^{Confetti} allele combined with *Nkx2.1*^{CreERT2}, *Id2*^{CreERT2}, and *Sftpc*^{CreERT2} mice were injected with 10 μg/g, 25 μg/g, and 5 μg/g per mouse, respectively. The *R26R*^{EYFP} or *R26R*^{TdTomato} allele crossed with the *Sftpc*^{CreERT2} or *Hopx*^{CreERT} mice were administered 100 μg/g per mouse. Dosing for clonal analysis in the *Hopx*^{CreERT}:*R26R*^{EYFP} mouse was 50 μg/g given to pregnant dams. Recombination in the *Hopx*$^{FlpOERT2/+}$:*Sftpc*^{CreERT2}:*R26R*$^{TdTom/+}$ mice was induced by using 100 μg/g.

SI Appendix includes further description of study materials and methods.

ACKNOWLEDGMENTS. We thank the technical support of the Penn Cardiovascular Institute Histology Core for their services; Florin Tuloc and his staff at the Flow Cytometry Core and Renata Pellegrino and Fernanda Mafra for scRNA-seq support at the Center for Applied Genomics at Children's Hospital of Philadelphia; Jonathan A. Epstein and Arun Padmanabhan for input and support in the generation of new reagents; and Andrea Stout (Penn Microscopy Core) for imaging support. This work was supported by National Institutes of Health Grants T32-HL007915, K12-HD043245, K08-HL140129 (to D.B.F.), DP2-HL147123 (to R.J.), F31-HL140785 (to I.J.P.), T32-HL007843 (to J.A.Z.), T32-HL007586 (to W.J.Z.), HL110942, HL132999, HL129478, and HL134745 (to E.E.M.); the Parker B. Francis Foundation (D.B.F.); the Pulmonary Hypertension Association (D.B.F.); the Burroughs Wellcome Career Award for Medical Scientists (to R.J.); National Science Foundation Grant CMMI-1548571 (to R.J. and R.L.-S.); and the Gilead Research Scholars Program (to R.J.).

1. Loh KM, et al. (2016) Mapping the pairwise choices leading from pluripotency to human bone, heart, and other mesoderm cell types. *Cell* 166:451–467.
2. Swarr DT, Morrisey EE (2015) Lung endoderm morphogenesis: Gasping for form and function. *Annu Rev Cell Dev Biol* 31:553–573.
3. Alanis DM, Chang DR, Akiyama H, Krasnow MA, Chen J (2014) Two nested developmental waves demarcate a compartment boundary in the mouse lung. *Nat Commun* 5:3923.
4. Chang DR, et al. (2013) Lung epithelial branching program antagonizes alveolar differentiation. *Proc Natl Acad Sci USA* 110:18042–18051.
5. Perl AK, Kist R, Shan Z, Scherer G, Whitsett JA (2005) Normal lung development and function after Sox9 inactivation in the respiratory epithelium. *Genesis* 41:23–32.
6. Rawlins EL, Clark CP, Xue Y, Hogan BL (2009) The Id2+ distal tip lung epithelium contains individual multipotent embryonic progenitor cells. *Development* 136: 3741–3745.
7. Rockich BE, et al. (2013) Sox9 plays multiple roles in the lung epithelium during branching morphogenesis. *Proc Natl Acad Sci USA* 110:E4456–E4464.
8. Miyamoto T, et al. (2002) Myeloid or lymphoid promiscuity as a critical step in hematopoietic lineage commitment. *Dev Cell* 3:137–147.
9. Laslo P, et al. (2006) Multilineage transcriptional priming and determination of alternate hematopoietic cell fates. *Cell* 126:755–766.
10. Akashi K, et al. (2003) Transcriptional accessibility for genes of multiple tissues and hematopoietic lineages is hierarchically controlled during early hematopoiesis. *Blood* 101:383–389.
11. Hu M, et al. (1997) Multilineage gene expression precedes commitment in the hemopoietic system. *Genes Dev* 11:774–785.
12. Enver T, Greaves M (1998) Loops, lineage, and leukemia. *Cell* 94:9–12.
13. Nestorowa S, et al. (2016) A single-cell resolution map of mouse hematopoietic stem and progenitor cell differentiation. *Blood* 128:e20–e31.
14. Paul F, et al. (2015) Transcriptional heterogeneity and lineage commitment in myeloid progenitors. *Cell* 163:1663–1677.
15. Rodriguez-Fraticelli AE, et al. (2018) Clonal analysis of lineage fate in native haematopoiesis. *Nature* 553:212–216.
16. Velten L, et al. (2017) Human haematopoietic stem cell lineage commitment is a continuous process. *Nat Cell Biol* 19:271–281.
17. Carrelha J, et al. (2018) Hierarchically related lineage-restricted fates of multipotent haematopoietic stem cells. *Nature* 554:106–111.
18. Pietras EM, et al. (2015) Functionally distinct subsets of lineage-biased multipotent progenitors control blood production in normal and regenerative conditions. *Cell Stem Cell* 17:35–46.
19. Yamamoto R, et al. (2013) Clonal analysis unveils self-renewing lineage-restricted progenitors generated directly from hematopoietic stem cells. *Cell* 154:1112–1126.
20. Desai TJ, Brownfield DG, Krasnow MA (2014) Alveolar progenitor and stem cells in lung development, renewal and cancer. *Nature* 507:190–194.
21. Treutlein B, et al. (2014) Reconstructing lineage hierarchies of the distal lung epithelium using single-cell RNA-seq. *Nature* 509:371–375.
22. Frank DB, et al. (2016) Emergence of a wave of Wnt signaling that regulates lung alveologenesis by controlling epithelial self-renewal and differentiation. *Cell Rep* 17: 2312–2325.
23. Chapman HA, et al. (2011) Integrin $\alpha 6\beta 4$ identifies an adult distal lung epithelial population with regenerative potential in mice. *J Clin Invest* 121:2855–2862.
24. Jain R, et al. (2015) Plasticity of Hopx(+) type I alveolar cells to regenerate type II cells in the lung. *Nat Commun* 6:6727.
25. Liebler JM, et al. (2016) Combinations of differentiation markers distinguish subpopulations of alveolar epithelial cells in adult lung. *Am J Physiol Lung Cell Mol Physiol* 310:L114–L120.
26. Wang Y, et al. (2018) Pulmonary alveolar type I cell population consists of two distinct subtypes that differ in cell fate. *Proc Natl Acad Sci USA* 115:2407–2412.
27. Yang J, et al. (2016) The development and plasticity of alveolar type 1 cells. *Development* 143:54–65.
28. Takeda N, et al. (2013) Hopx expression defines a subset of multipotent hair follicle stem cells and a progenitor population primed to give rise to K6+ niche cells. *Development* 140:1655–1664.
29. Li D, et al. (2015) Hopx distinguishes hippocampal from lateral ventricle neural stem cells. *Stem Cell Res (Amst)* 15:522–529.
30. Barkauskas CE, et al. (2013) Type 2 alveolar cells are stem cells in adult lung. *J Clin Invest* 123:3025–3036.
31. Snippert HJ, et al. (2010) Intestinal crypt homeostasis results from neutral competition between symmetrically dividing Lgr5 stem cells. *Cell* 143:134–144.
32. Tiozzo C, et al. (2009) Deletion of Pten expands lung epithelial progenitor pools and confers resistance to airway injury. *Am J Respir Crit Care Med* 180:701–712.
33. Taniguchi H, et al. (2011) A resource of Cre driver lines for genetic targeting of GABAergic neurons in cerebral cortex. *Neuron* 71:995–1013.
34. Darmanis S, et al. (2016) Simultaneous multiplexed measurement of RNA and proteins in single cells. *Cell Rep* 14:380–389.
35. Vogel C, Marcotte EM (2012) Insights into the regulation of protein abundance from proteomic and transcriptomic analyses. *Nat Rev Genet* 13:227–232.
36. Brunskill EW, et al. (2014) Single cell dissection of early kidney development: Multilineage priming. *Development* 141:3093–3101.
37. Kim TH, et al. (2016) Single-cell transcript profiles reveal multilineage priming in early progenitors derived from Lgr5(+) intestinal stem cells. *Cell Rep* 16:2053–2060.
38. Longmire TA, et al. (2012) Efficient derivation of purified lung and thyroid progenitors from embryonic stem cells. *Cell Stem Cell* 10:398–411.
39. Qiu X, et al. (2017) Reversed graph embedding resolves complex single-cell trajectories. *Nat Methods* 14:979–982.
40. Madisen L, et al. (2015) Transgenic mice for intersectional targeting of neural sensors and effectors with high specificity and performance. *Neuron* 85:942–958.
41. Lescroart F, et al. (2018) Defining the earliest step of cardiovascular lineage segregation by single-cell RNA-seq. *Science* 359:1177–1181.
42. Kattman SJ, Huber TL, Keller GM (2006) Multipotent flk-1+ cardiovascular progenitor cells give rise to the cardiomyocyte, endothelial, and vascular smooth muscle lineages. *Dev Cell* 11:723–732.
43. Kattman SJ, et al. (2011) Stage-specific optimization of activin/nodal and BMP signaling promotes cardiac differentiation of mouse and human pluripotent stem cell lines. *Cell Stem Cell* 8:228–240.
44. Moretti A, et al. (2006) Multipotent embryonic isl1+ progenitor cells lead to cardiac, smooth muscle, and endothelial cell diversification. *Cell* 127:1151–1165.
45. Wu SM, et al. (2006) Developmental origin of a bipotential myocardial and smooth muscle cell precursor in the mammalian heart. *Cell* 127:1137–1150.
46. Devine WP, Wythe JD, George M, Koshiba-Takeuchi K, Bruneau BG (2014) Early patterning and specification of cardiac progenitors in gastrulating mesoderm. *eLife* 3: e03848.
47. Lescroart F, et al. (2014) Early lineage restriction in temporally distinct populations of Mesp1 progenitors during mammalian heart development. *Nat Cell Biol* 16:829–840.
48. Waddington CH (1940) *Organisers & Genes* (Cambridge Univ Press, Cambridge, UK).
49. Jain R, Epstein JA (2018) Competent for commitment: You've got to have heart! *Genes Dev* 32:4–13.
50. Jensen KB, et al. (2009) Lrig1 expression defines a distinct multipotent stem cell population in mammalian epidermis. *Cell Stem Cell* 4:427–439.
51. Gotoh S, et al. (2014) Generation of alveolar epithelial spheroids via isolated progenitor cells from human pluripotent stem cells. *Stem Cell Reports* 3:394–403.
52. Huang SX, et al. (2015) The in vitro generation of lung and airway progenitor cells from human pluripotent stem cells. *Nat Protoc* 10:413–425.
53. Jacob A, et al. (2017) Differentiation of human pluripotent stem cells into functional lung alveolar epithelial cells. *Cell Stem Cell* 21:472–488.e10.
54. Zacharias WJ, et al. (2018) Regeneration of the lung alveolus by an evolutionarily conserved epithelial progenitor. *Nature* 555:251–255.
55. Pei W, et al. (2017) Polylox barcoding reveals haematopoietic stem cell fates realized in vivo. *Nature* 548:456–460.
56. Biddy BA, et al. (2018) Single-cell mapping of lineage and identity in direct reprogramming. *Nature* 564:219–224.
57. Li J, et al. (2018) The strength of mechanical forces determines the differentiation of alveolar epithelial cells. *Dev cell* 44:297–312.e5.
58. Arnold K, et al. (2011) Sox2(+) adult stem and progenitor cells are important for tissue regeneration and survival of mice. *Cell Stem Cell* 9:317–329.
59. Madisen L, et al. (2010) A robust and high-throughput Cre reporting and characterization system for the whole mouse brain. *Nat Neurosci* 13:133–140.